

Article

Elastic Critical Lateral Buckling of Beams Subjected to Simultaneous Negative End Moments and Transverse Loads

Xuan Tung Nguyen ¹, Tri N. M. Nguyen ¹, Kha Loc Nguyen ¹, Ki-Yong Yoon ², Sun-Hee Park ³
and Jung J. Kim ^{4,*}

¹ Campus in Ho Chi Minh City, University of Transport and Communications, Ho Chi Minh City 700000, Vietnam

² Department of Civil Infrastructure Systems and Safety Engineering, Sunmoon University, Asan 31460, Republic of Korea

³ R&D Department, Kwang Deug E&C, Gumi 39454, Republic of Korea

⁴ Department of Civil Engineering, Kyungnam University, Changwon-si 51767, Republic of Korea

* Correspondence: jungkim@kyungnam.ac.kr; Tel.: +82-55-249-6421; Fax: +82-505-999-2165

Abstract: This study presents a numerical investigation of the elastic critical lateral-torsional buckling of a steel beam subjected to simultaneous transverse loading at the top flange and negative end moments. Here, the elastic critical buckling of the steel beam was estimated by utilizing the finite element software ABAQUS. In addition, the influence of the length-to-height ratio was taken into account. Additionally, the predicted values for elastic critical buckling when applying existing design codes and a previous study were also analyzed and compared to the numerical results of the finite element analysis. The result of the comparison revealed that the projected values from the design codes and the study are conservative for the majority of cases and have a tendency to be too conservative when the length-to-height ratio increases. Furthermore, a new equation with a factor considering the influence of the length-to-height ratio and transverse loading on the top flange is proposed, and the proposed equation shows sufficient accuracy and less conservative values for most cases.

Keywords: finite element analysis; elastic critical buckling; length-to-height ratio; transverse loading; negative end moment



Citation: Nguyen, X.T.; Nguyen, T.N.M.; Nguyen, K.L.; Yoon, K.-Y.; Park, S.-H.; Kim, J.J. Elastic Critical Lateral Buckling of Beams Subjected to Simultaneous Negative End Moments and Transverse Loads. *Appl. Sci.* **2023**, *13*, 778. <https://doi.org/10.3390/app13020778>

Academic Editors: Angelo Luongo and Simona Di Nino

Received: 3 December 2022

Revised: 22 December 2022

Accepted: 23 December 2022

Published: 5 January 2023



Copyright: © 2023 by the authors. Licensee MDPI, Basel, Switzerland. This article is an open access article distributed under the terms and conditions of the Creative Commons Attribution (CC BY) license (<https://creativecommons.org/licenses/by/4.0/>).

1. Introduction

Overhanging beams and continuous beams are common structures in buildings and bridges, which are directly subjected to transverse loadings, resulting in negative moments occurring at interior supports, as shown in Figure 1. For flexural steel members, the loss of stability of lateral-torsional buckling (LTB) is a common failure phenomenon. Moreover, elastic moment determination to predict the buckling strength values of steel beams must be performed and checked as one ultimate limit state considered to be one of the critical standards, which can be found in several current design standards and guidelines [1–6]. However, so far, many researchers have proven that the recommendations of some standards and guidelines are too conservative or even unsafe under specified conditions, which has to be investigated in detail under particular circumstances to ensure the economic and safety indicators. Based on many previous studies, a buckling resistance evaluation greatly depends on two factors, bending moment distribution and restriction at supports, which have been widely numerically investigated by many researchers under several specified investigated factors.

Theoretical studies on the elastic critical buckling of steel beams have been carried out in many works in the literature, wherein studies on the elastic buckling of simply supported steel beams with a monosymmetric cross-section subjected to transverse loadings or end moments were presented in [7–9]. Here, Kitipornchai and Wang [7], Kitipornchai et al. [8]

and Wang and Kitipornchai [9] revealed that the proposed design graphs are different from current design solutions in which the moment gradient factor (C_b) is employed. In addition, Lim et al. [10] also investigated the elastic lateral-torsional buckling utilizing an I-beam and applying the Bubnov–Galerkin method [11] and the finite element method. The authors developed alternative equations concerning the C_b correction factor and the end constraint boundary conditions. As a result, in three end restraint cases, more precise solutions were attained with greater safety and less conservative values over the entire selection of linear moment gradients in the three above-mentioned cases.

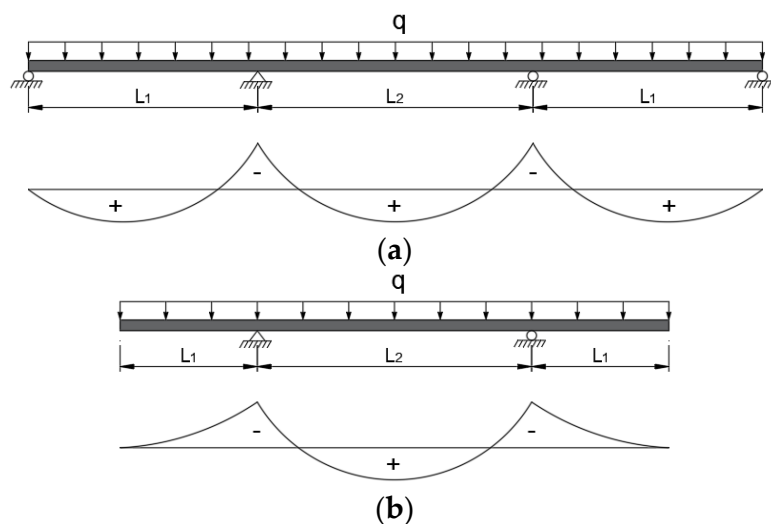


Figure 1. Bending moment diagram. (a) Continuous beam, (b) Overhanging beam.

In addition, studies on beams subjected to simultaneous transverse loadings and end moments were also carried out in [12–15]. As a result, the moment gradient factors based on the bending diagram were proposed. The equivalent uniform moment factor (EUMF) method was investigated by Serna et al. [14]. The results indicated, in the case of simply supported beams with very conservative values, additionally, non-conservative values occurred when support types were used to limit lateral bending and warping. Furthermore, the investigation of Wong et al. [15] also revealed unacceptable results for a procedure from a design standard [16], for most cases taking into account common bending moment distributions considering the moment gradient factor values observed from twelve moment distribution comparisons. Moreover, a proposed equation was proven to be appropriate for most cases of typical applications; however, the equation does not show good agreement when concentrated loads occur, as with all quarter-point moment methods.

In terms of the impact of the loading position in cross-sectional depth on the elastic critical buckling of the beam, it has been also studied in [17–20]. Generally, these studies have considered the shape of the cross-section, including singly and doubly symmetric cross-sections. The effect of loading conditions, including beams subjected to end moments and transverse loadings, as well as the effect of load heights on the elastic critical LTB were also taken into account. The study of Park et al. [19] compared the results from the SSRC Guide [6] with the results of the FEA method, leading to a new design method restricted in cases of monosymmetric I-beams with a monosymmetric degree ranging between 0.1 and 0.9. Moreover, Bijak [20] studied the analysis of unbraced, symmetric, prismatic beams of simply supported ones in terms of the lateral-torsional critical moment, proving an incorrect estimation in a previous study [21] in terms of the coefficient allowing for random ordinates of applied loadings. Moreover, the study also investigated the assumption of boundary conditions, non-linear bending moment distributions and the impact of the position of loading concerning the height of the cross-sectional element.

On the other hand, Park et al. [22] and Park [23] numerically investigated the effect of the length-to-height ratio on the LTB of stepped beams with a continuously laterally

braced top flange. In the studies, the loading conditions on stepped beam models were a concentrated load at midspan and a uniformly distributed load on the top flange with negative end moments. As a result, the data of these studies showed that the length-to-height ratio has a great influence on the LTB of stepped beams with continuous lateral bracing.

Recently, cellular beams have been investigated and widely applied, with several advantages compared to conventional solid web steel beams. The numerical investigation of their elastic buckling behavior has been considered by several researchers [24–28], with the modified factors considering the presence of web perforations under specified conditions. In this case, the study by Khatri et al. [28] investigated the impact of load height on the C_b factor under uniform load distribution for laterally unsupported I-beams. The C_b factor attained from the numerical results was compared with the procedure calculations from SSRC guidance, leading to considerable variation between these results, which was due to serious web distortion, which is neglected in the equations in the SSRC guidance. Moreover, the application of this guidance is appropriate when the mode of lateral-torsional buckling is dominant for span beams that are longer than the investigated one.

To date, there have been many standards and guidelines [1–6] aimed at preventing the lateral-torsional buckling phenomenon; however, as mentioned above, these recommendations are either too conservative or unsafe in some circumstances. Moreover, although the elastic critical buckling of steel beams has been focused on and researched with many proposed models to analyze the related ultimate limit stage under specific circumstances, to the best of our knowledge, the effect of the length-to-height ratio with transverse loads at the top flange on the elastic critical LTB of prismatic steel beams has been studied with limitations in the literature. Therefore, this paper focuses on the investigation of the influence of the length-to-height ratio on the elastic critical buckling of prismatic steel I-beams. The simply supported beams were subjected to a uniformly distributed load or concentrated load on the top flange with negative end moments. In addition, a finite element program (ABAQUS) was employed to analyze the elastic critical buckling of beam models. Eventually, an equation was proposed, compared and verified with several standards and a previous study. As a result, the proposed equation indicated good agreement, with less conservative values compared to the previous study and the standards for most cases.

2. Background and Previous Research

Timoshenko and Gere [29] provided the equation to calculate the elastic critical LTB for a doubly symmetric I-beam under equal end moments as follows:

$$M_{ocr} = \frac{\pi}{L} \sqrt{EI_y GJ + \left(\frac{\pi E}{L}\right)^2 I_y C_w} \quad (1)$$

where L is the unbraced length; E and G are the Young's modulus and the shear modulus, respectively; I_y is the inertia moment of the cross-section about the minor axis; J and C_w are the torsional and warping constants, respectively.

In order to take into account the influence of varying bending moments within the laterally unbraced length, a moment gradient factor (C_b) was proposed. Moreover, the elastic critical LTB strength of beams subjected to general loading conditions (M_{cr}) is also calculated by multiplying M_{ocr} by C_b based on the study of Salvadori [30]. The author offered a moment modification factor that has been also incorporated into the American Institute of Steel Construction (AISC) Specifications (1986) [5]:

$$C_b = 1.75 + 1.05 \left(\frac{M_2}{M_1}\right) + 0.3 \left(\frac{M_2}{M_1}\right)^2 \quad (2)$$

in which M_1 and M_2 are the greater and smaller end moments, respectively. In addition, the value of the ratio M_2/M_1 is taken as negative for end moments triggering single-curvature bending and positive for end moments causing double-curvature bending. It should be

noted that Equation (2) was developed for the case of beams subjected to end moments without transverse loadings.

The moment gradient factor was established by Kirby and Nethercot [12], which has been also incorporated into the AISC Specifications (2016) [1]:

$$C_b = \frac{12.5M_{max}}{2.5M_{max} + 3M_A + 4M_B + 3M_C} \quad (3)$$

where M_{max} is the absolute value of the maximum moment; M_A , M_B and M_C are the absolute values of the moments at the quarter point, the center point and the three-quarter point, respectively. It should be mentioned that this factor can be applied to bending moment diagrams of any shape. Moreover, the loads are imposed at the shear center of the cross-section.

BS 5950 [4] provides the equation for the moment correction factor given by

$$C_b = \frac{M_{max}}{0.2M_{max} + 0.15M_A + 0.5M_B + 0.15M_C} \leq 2.273 \quad (4)$$

The equation of C_b used in the AS 4100 [2] is taken as

$$C_b = \frac{1.7M_{max}}{\sqrt{M_A^2 + M_B^2 + M_C^2}} \leq 2.5 \quad (5)$$

The position of the transverse loading in the cross-sectional depth also influences the elastic critical LTB strength of the beam. Helwig et al. [17] suggested a simplified formula for the moment gradient factor of simply supported beams, as presented in Equation (6), which has been also mentioned in Ziemian [6]:

$$C_b^* = (1.4^{2y/h})C_b \quad (6)$$

where C_b is determined using Equation (3); h is the beam height; y is the distance from the midheight of the cross-section to the transverse loading position. Furthermore, the value of y is negative for transverse loading above the midheight and positive for transverse loading below the midheight.

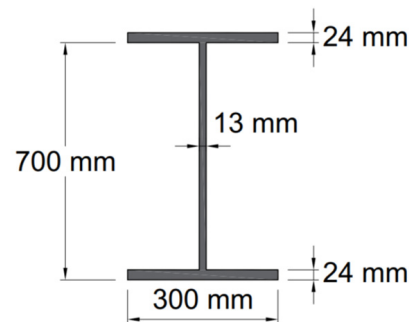
Moreover, there are also studies on the moment gradient factor for the elastic critical LTB of steel beams, which were performed by Serna et al. [14] and Wong and Driver [15]. In their studies, the factor C_b was also used only for the case of transverse loadings imposed at the shear center of the cross-section. For this study, the factor C_b for steel beams subjected to transverse loadings on top flanges with negative end moments is followed, according to the recommendations from the investigation of Helwig et al. [17] and Ziemian [6].

3. Finite Element Modeling

The elastic critical LTB of steel beams subjected to transverse loading with negative end moments was achieved using the finite element analysis (FEA) program ABAQUS [31], applying the four-node shell element (S4R), which was utilized to model the investigated steel beam. It should be mentioned that the S4R element, with six degrees of freedom at each node, which was also used in previous studies [32–37], can accurately model the elastic buckling behavior of steel beams and provide quick results with high accuracy. In addition, the steel beam with an H700x300 cross-section was chosen in this study according to [38], with detailed properties listed in Table 1. Regarding the cross-section size of the beams, the beam height (h), flange width (b_f), flange thickness (t_f) and web thickness (t_w) were 700, 300, 24 and 13 mm, respectively, as shown in Figure 2. In addition, the mechanical properties of the beams, i.e., elastic modulus (E) and yield stress (f_y), are 210 and 275 Mpa, respectively. Meanwhile, the Poisson's ratio (m) was 0.3, and all the geometric and mechanical properties of the beams were taken from [38].

Table 1. Properties of H700x300 (unit: mm, MPa).

Properties	Values
Beam height, h	700
Flange width, b_f	300
Flange thickness, t_f	24
Web thickness, t_w	13
Elastic modulus, E	210
Yield stress, f_y	275
Poisson's ratio, m	0.3

**Figure 2.** Cross-section of beams.

In order to consider the various beam lengths, a range of length-to-height ratios (L/h) from 10 to 40 with an interval of 5 was employed. Moreover, a convergence analysis was conducted to determine the proper mesh size of the steel beam models. Furthermore, based on the analysis results, the meshing of beam models was achieved with $30 \text{ mm} \times 30 \text{ mm}$ elements. The elastic critical LTB of steel beams was investigated by using eigenvalue analyses.

This study aimed to investigate the LTB strength of simply supported beams subjected to transverse loadings on top flanges with negative end moments. In addition, the beam model and boundary condition of the simply supported beam are given in Figure 3. Here, both tips of the bottom flanges and both centroids at the ends of the web were fixed to ensure the prevention of vertical displacements. Likewise, lateral displacements for both tips of the web were also prevented. Moreover, the displacement along the axial direction of one centroid at the ends of the web was prevented for the hinge support and another one was free at the position of the roller support.

Figure 4 shows the loading conditions used in this study. It can be seen that the steel beams were subjected to a uniformly distributed load or concentrated load on the top flange with negative end moments, which are denoted LC_1 and LC_2 , respectively. In Figure 4, M_1 and M_2 are the greater and smaller moments at the ends of the beam, and α is the ratio of M_1 taking into account the end moment variation with the values of α as 0, 0.5, 0.75 and 1. In addition, M_q and M_p are, respectively, the moment at the midspan of the simple beam triggered by the uniformly distributed load and the concentrated load with respect to unbraced length L . To take into account the effect of the variation in the negative end moments and transverse loadings, the M_q/M_1 and M_p/M_1 ratios were investigated ranging from 0.5 to 3 with an interval of 0.5 in this study.

The negative end moments were simulated by using tension forces at the top flange and compression forces at the bottom flange, as shown in Figure 5. In addition, the typical buckling mode shapes are illustrated in Figure 6. Additionally, for the case of the M_q/M_1 and M_p/M_1 ratios greater than 1, the buckling of the beam occurs in the top flange, as shown in Figure 6a. In the case of M_q/M_1 and M_p/M_1 ratios less than 1, the buckling of the beam occurs in the bottom flange (i.e., compression flange), as shown in Figure 6b.

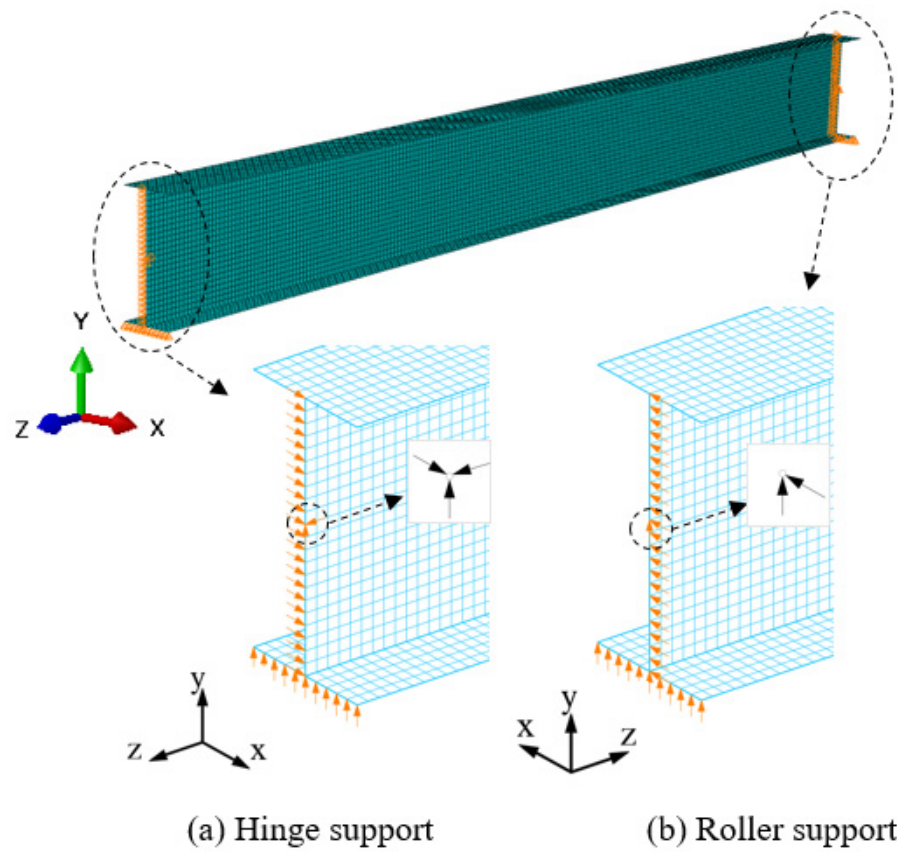


Figure 3. Beam model and boundary conditions.

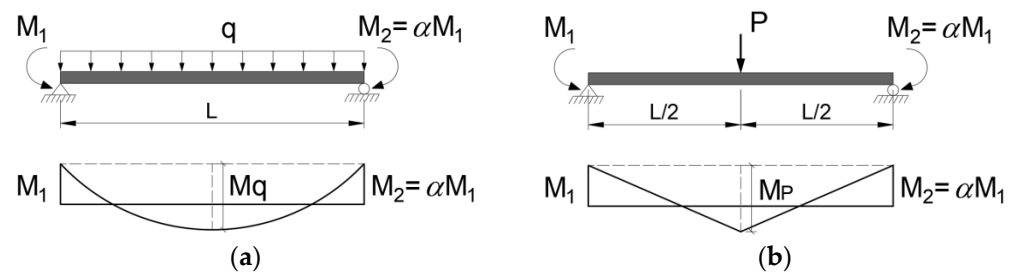


Figure 4. Loading conditions. (a) LC₁, (b) LC₂.

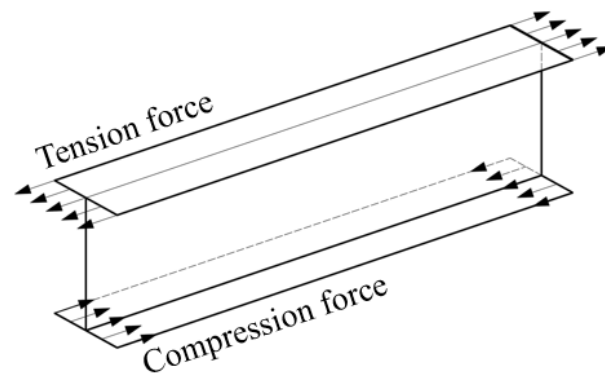


Figure 5. End moment simulation.

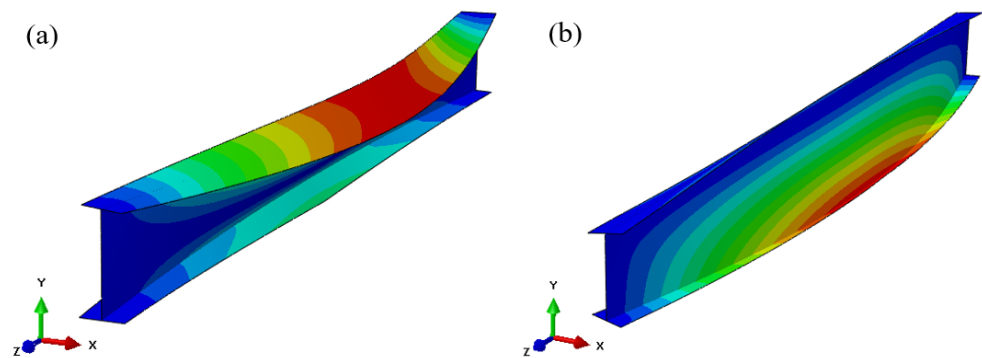


Figure 6. Typical buckling mode shapes. (a) $M_{q(P)}/M_1 > 1$, (b) $M_{q(P)}/M_1 \leq 1$.

Table 2 presents the elastic critical buckling strengths of these beams subjected to equal end moments. The data show that the elastic critical buckling strengths obtained in the FEA and Timoshenko and Gere's study [29] are in very good agreement.

Table 2. Comparison between Timoshenko and Gere's study and FEA.

L/h	Elastic Critical Moment (kN.m)		Difference (%)
	Timoshenko and Gere [29]	FEA	
10	1894.96	1891.12	−0.20
15	1003.31	996.84	−0.65
20	670.97	663.96	−1.06
25	503.75	497.04	−1.35
30	404.05	397.88	−1.55
35	337.94	332.32	−1.69
40	290.83	285.72	−1.79

4. Finite Element Results

A total of 336 models were analyzed to investigate the effect of the length-to-height ratio (L/h) on the elastic critical LTB of steel beams. For this, simply supported beams were simultaneously subjected to negative end moments and transverse loadings on the top flanges. As mentioned, the values of the ratio of L/h from 10 to 40 with an interval of 5 were used. In addition, values of α from 0 to 1 and M_q/M_1 and M_p/M_1 ratios ranging from 0.5 to 3 with an interval of 0.5 were considered.

Figures 7 and 8 show the FEA results for steel beams with LC₁ and LC₂, respectively. The representative cases with α of 0 and 1, corresponding to the cases of one negative end moment and negative end equal moments, are presented. Moreover, the results are presented as the ratio of the elastic critical buckling of beams with LC₁ and LC₂, M_{cr} , to the elastic critical buckling of beams subjected to end equal moments, M_{ocr} , with respect to M_q/M_1 or M_p/M_1 . Obviously, these figures show that the ratio of M_{cr}/M_{ocr} for beams with LC₁ and LC₂ increases as the ratio of L/h increases. As can be seen from the figures, the data also indicate that the values of M_{cr}/M_{ocr} are greater than 1 and change with the shape of the bending moment diagrams. In the case of $\alpha = 0$, the ratio of M_{cr}/M_{ocr} gradually decreases as the $M_{q(P)}/M_1$ ratio increases for both LC₁ and LC₂, as shown in Figures 7a and 8a, respectively. In the case of $\alpha = 1$, the ratio of M_{cr}/M_{ocr} increases when $M_{q(P)}/M_1$ is less than 1. The ratio of the M_{cr}/M_{ocr} ratio gradually decreases when the M_q/M_1 ratio is greater than 1, as shown in Figures 7b and 8b.

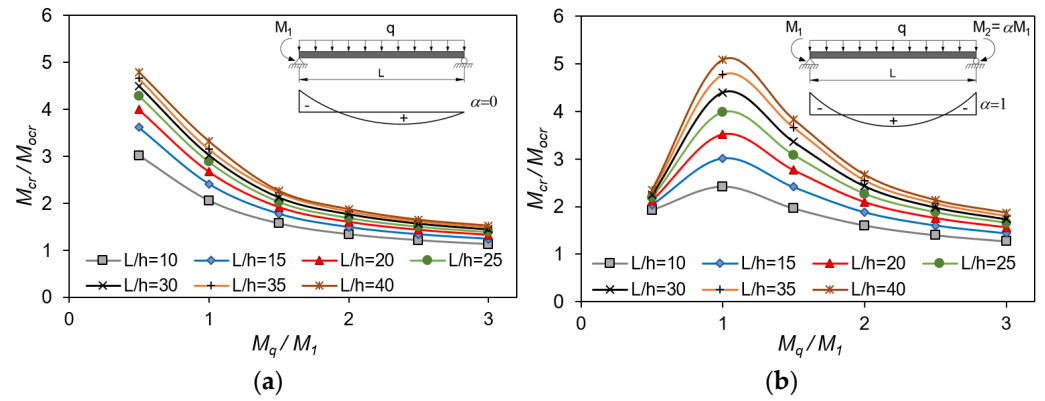


Figure 7. Finite element analysis results for LC₁. (a) $\alpha = 0$. (b) $\alpha = 1$.

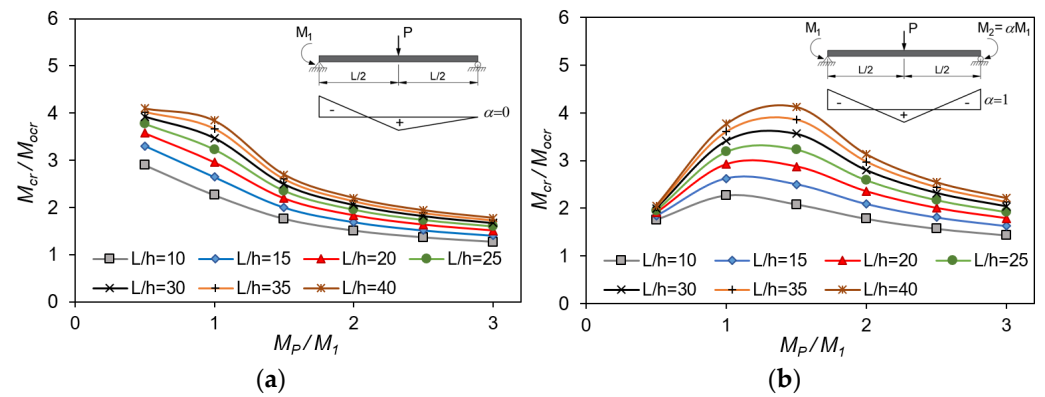


Figure 8. Finite element analysis results for LC₂. (a) $\alpha = 0$. (b) $\alpha = 1$.

5. Proposed Equation

To consider the effect of different loading conditions, the moment gradient factor is multiplied by the values of M_{ocr} . In addition, the existing equations for calculating the moment gradient factor are taken from Equations (3)–(6) and correspond to the recommendations of AISC [1], BS 5950 [4], AS 4100 [2] and the study of Helwig et al. [17]. Moreover, Figures 9 and 10 show comparisons of the elastic critical buckling of beams with LC₁ and LC₂, respectively, between the FEA results and the existing equations. It can be seen that the estimated values using the recommendations of the standards AISC, BS5950 and AS4100 are conservative for most cases and tend to be too conservative as the L/h ratio increases. In addition, there are also a few cases of small values of L/h (i.e., L/h of 10, 15) with unconservative and acceptable results. Moreover, Helwig’s study provides too conservative results for all models, which increase as the L/h ratio increases, as shown in Figures 9d and 10d. Furthermore, the standards of AISC, BS 5950, AS 4100 and Helwig’s study give maximum differences for conservative values of 50.7%, 59.3%, 55.3% and 64.8%, respectively. Additionally, the maximum differences for unconservative values are -35.4% , -4.6% and -27.4% for AISC (2016), BS 5950 and AS 4100, respectively.

In order to increase the accuracy, a proposed equation was developed for the elastic critical buckling of steel beams subjected to simultaneous transverse loadings at the top flange and negative end moments as follows:

$$M_{cr} = F_b C_b M_{ocr} \tag{7}$$

in which M_{ocr} is the elastic critical buckling of beams subjected to equal end moments and is calculated using Equation (1); C_b is given in AISC 2016 and in Equation (3) and has been widely used in previous studies; F_b is the factor considering the length-to-height ratio (L/h) and transverse loading on the top flange. Based on the FEA results, the proposal for F_b was

developed as a set of linear expressions and is defined in Table 3, in which the expressions of F_b were developed for LC₁ and LC₂ based on the ratio between M_1 and M_2 , including the cases of beams subjected to transverse loading on the top flange with one negative end moment (i.e., $\alpha = 0$) and two negative end moments (i.e., $0 < \alpha \leq 1$).

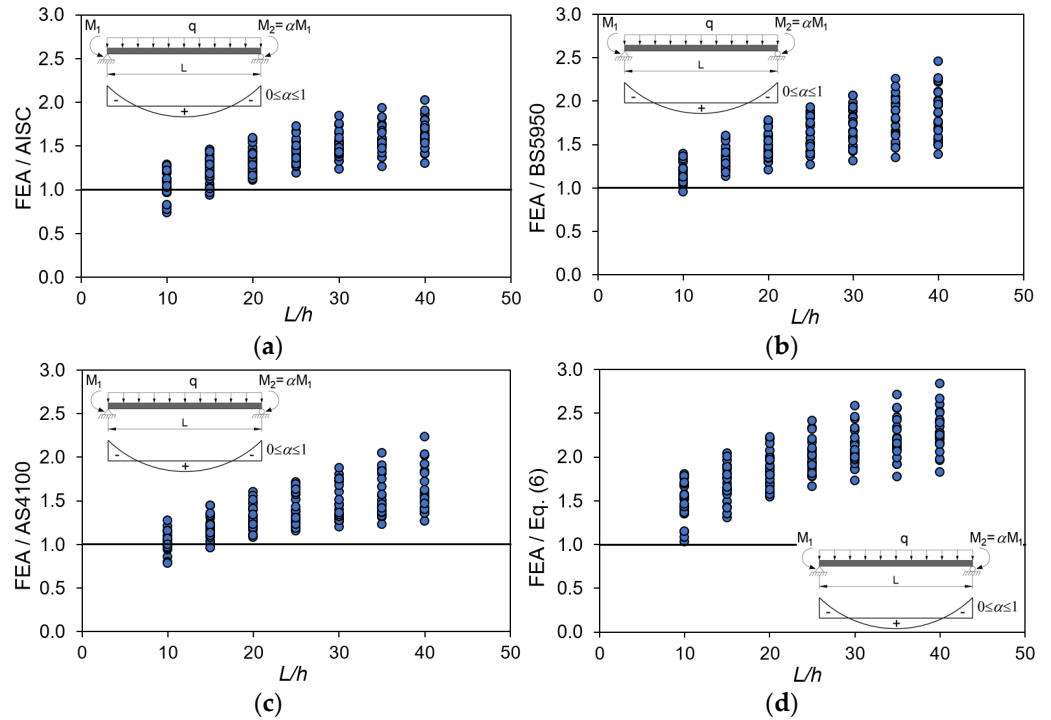


Figure 9. Comparison of elastic critical LTB for LC₁ between FEA results and existing equations. (a) AISC [1], (b) BS 5950 [4], (c) AS 4100 [2], (d) Helwig’s study [17].

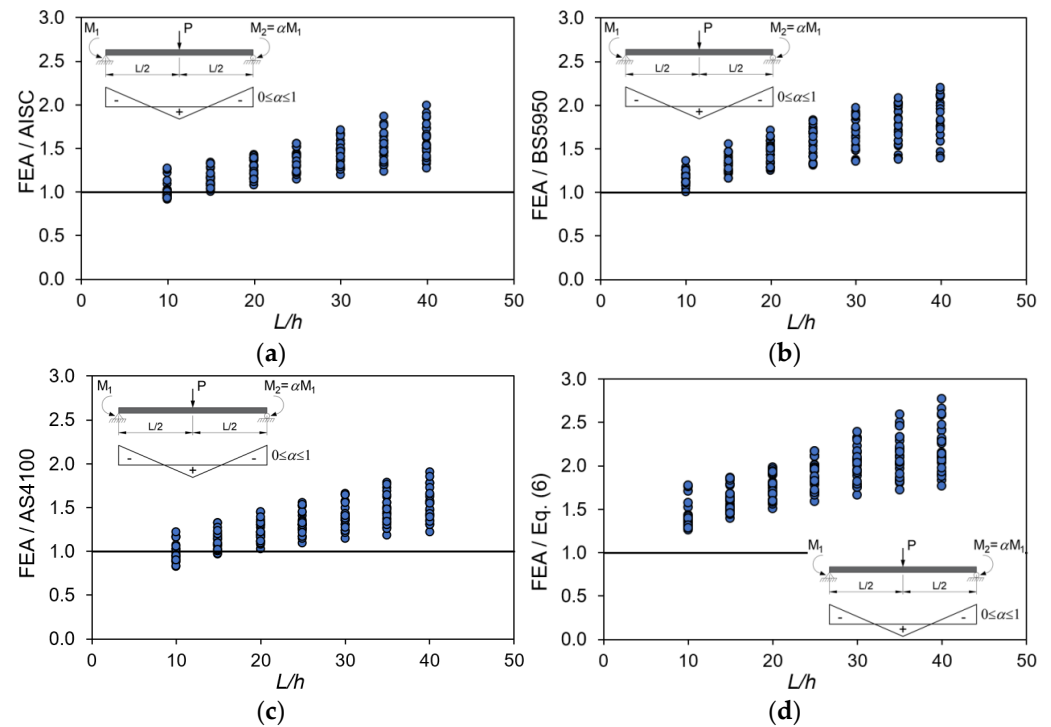


Figure 10. Comparison of elastic critical LTB for LC₂ between FEA results and existing equations. (a) AISC [1], (b) BS 5950 [4], (c) AS 4100 [2], (d) Helwig’s study [17].

Table 3. F_b factor.

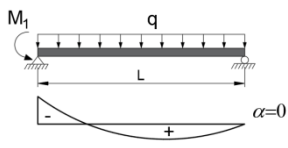
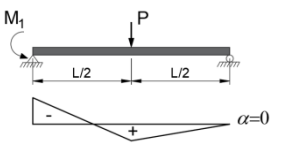
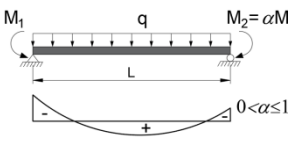
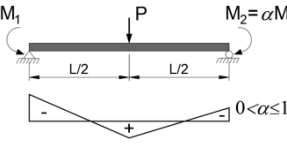
LC_1	LC_2	Value of α	F_b
		$\alpha = 0$	$\frac{L}{85h} + 0.8$
		$0 < \alpha \leq 1$	$\frac{L}{75h} + 0.8$

Figure 11a,b present the comparison between the FEA results and the proposed equation for LC_1 and LC_2 , respectively. Evidently, it can be observed that the proposed equation gives reasonable accuracy and less conservative values compared to Figures 8 and 9, with the results taken from the standards and the study. In addition, the proposed equation provides conservative values for most cases, with maximum differences of 35.1% and 32.7% for LC_1 and LC_2 , respectively. Moreover, only 3.3% of beam models provide unconservative values, with the maximum differences of -26.4% and -1.9% for LC_1 and LC_2 , respectively. In addition, Table 4 presents the peak differences between the FEA results and considered equations, with the positive and negative values indicating conservative and unconservative values, respectively.

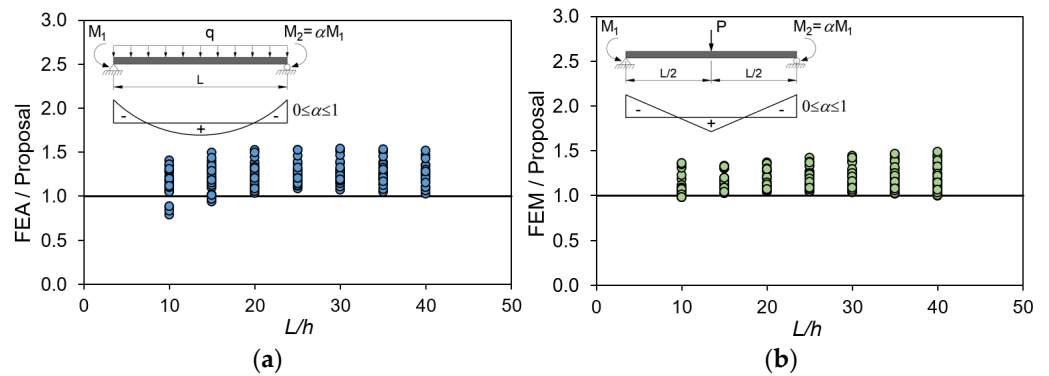


Figure 11. Comparison of elastic critical LTB between FEA results and proposed equations. (a) LC_1 , (b) LC_2 .

Table 4. Differences in elastic critical LTB between FEA and considered equations.

Design Equation	LC_1		LC_2	
	Maximum	Minimum	Maximum	Minimum
AISC	50.7%	-35.4%	49.5%	-10.1%
BS 5950	59.3%	-4.6%	54.36%	-0.1%
AS 4100	55.3%	-27.4%	47.4%	-22.5%
Helwig’s study	64.8%	3.31%	63.9%	20.9%
Proposed equation	35.1%	-26.4%	32.7%	-1.9%

6. Conclusions

This paper investigates the elastic critical buckling of prismatic steel beams subjected to transverse loadings at the top flange with negative end moments. In addition, the elastic critical buckling of steel beams was analyzed by using the FEA program ABAQUS. Here, 336 models in total were used to study the influence of the length-to-height ratio (L/h) on the elastic critical LTB of steel beams, and simply supported beams were simultaneously subjected to negative end moments and transverse loadings on the top flanges. In addition, the end moment variation was taken into account with the investigated end moment ratios of 0, 0.5, 0.75 and 1. Additionally, to consider the effect of the variation in the negative end moments and transverse loadings, the M_q/M_1 and M_P/M_1 ratios were considered, ranging between 0.5 and 3, with a gap of 0.5, applied in this study. After performing the comparisons between the FEA, existing designed procedures and Helwig's investigation, some conclusions can be drawn as follows:

1. The ratio of M_{cr}/M_{ocr} for beams with LC₁ and LC₂ increased as the ratio of L/h increased. The values of M_{cr}/M_{ocr} were greater than 1 and changed with the values of the $M_{q(P)}/M_1$ ratio.
2. The predicted values obtained from the current design standards and Helwig's study were conservative for most cases and tended to be too conservative as the L/h ratio increased. AISC 2016, BS 5950, AS 4100 and Helwig's study give maximum differences for conservative values of 50.7%, 59.3%, 55.3% and 64.8%, respectively.
3. A new equation with a factor, F_b , taking into account the effect of the length-to-height ratio and transverse loading on the top flange was proposed. The proposed equation provided reasonable accuracy and less conservative values for most cases, with maximum differences of 35.1% and 32.7% for LC₁ and LC₂, respectively.

Author Contributions: Conceptualization, J.J.K.; methodology, X.T.N. and J.J.K.; software, X.T.N. and S.-H.P.; validation, T.N.M.N. and K.L.N.; formal analysis, T.N.M.N., S.-H.P. and K.L.N.; investigation, X.T.N. and K.-Y.Y.; resources, J.J.K.; data curation, X.T.N. and T.N.M.N.; writing—original draft preparation, X.T.N., S.-H.P. and K.L.N.; writing—review and editing, T.N.M.N., S.-H.P. and J.J.K.; visualization, X.T.N. and K.L.N.; supervision, J.J.K. and K.-Y.Y.; project administration, J.J.K.; funding acquisition, K.-Y.Y. All authors have read and agreed to the published version of the manuscript.

Funding: This research was supported by a grant (RS-2021-KA163626) from the Technology Advancement Research Program (TARP) funded by the Ministry of Land, Infrastructure, and Transport of the Korean government.

Institutional Review Board Statement: Not applicable.

Informed Consent Statement: Not applicable.

Data Availability Statement: Data are contained within the article.

Conflicts of Interest: The authors declare no conflict of interest.

References

1. *ANSI/AISC 360-16*; Specification for Structural Steel Buildings. American Institute of Steel Construction: Chicago, IL, USA, 2016.
2. *AS 4100*; Steel Structures. Standards Australia: Homebush, NSW, Australia, 1998.
3. *EN 1993-1-1*; Design of Steel Structures Part 1–1: General Rules and Rules for Buildings. European Committee for Standardization (ECS): Brussels, Belgium, 2005.
4. *BS5950*; Structural Use of Steelwork in Building—Part 1: Code of Practice for Design—Rolled and Welded Sections. British Standards Institution: London, UK, 2000.
5. *AISC-86*; Load and Resistance Factor Design Specification for Structural Steel Buildings. American Institute of Steel Construction: Chicago, IL, USA, 1986.
6. Ziemian, R.D. *Guide to Stability Design Criteria for Metal Structures*, 6th ed.; John Wiley & Son, Inc.: Hoboken, NJ, USA, 2010.
7. Kitipornchai, S.; Wang, C.M. Lateral buckling of tee beams under moment gradient. *Comput. Struct.* **1986**, *23*, 69–76. [[CrossRef](#)]
8. Kitipornchai, S.; Wang, C.M.; Trahair, N.S. Buckling of monosymmetric I-beams under moment gradient. *J. Struct. Eng.* **1986**, *112*, 781–799. [[CrossRef](#)]
9. Wang, C.M.; Kitipornchai, S. Buckling capacities of monosymmetric I-beams. *J. Struct. Eng.* **1986**, *112*, 2373–2391. [[CrossRef](#)]

10. Lim, N.H.; Park, N.H.; Kang, Y.J.; Sung, I.H. Elastic buckling of I-beams under linear moment gradient. *Int. J. Solids Struct.* **2003**, *40*, 5635–5647. [[CrossRef](#)]
11. Khurshudyan, A.Z. The Bubnov–Galerkin method in control problems for bilinear systems. *Autom. Remote Control* **2015**, *76*, 1361–1368. [[CrossRef](#)]
12. Kirby, P.A.; Nethercot, D.A. *Design for Structural Stability*; John Wiley and Sons: New York, NY, USA, 1979.
13. Suryoatmono, B.; Ho, D. The moment-gradient factor in lateral–torsional buckling on wide flange steel sections. *J. Constr. Steel Res.* **2002**, *25*, 1247–1264. [[CrossRef](#)]
14. Serna, M.A.; López, A.; Puente, I.; Yong, D.J. Equivalent uniform moment factors for lateral–torsional buckling of steel members. *J. Constr. Steel Res.* **2006**, *62*, 566–580. [[CrossRef](#)]
15. Wong, E.; Driver, R.G. Critical evaluation of equivalent moment factor procedures for laterally unsupported beams. *Eng. J.* **2010**, *47*, 1–20.
16. CSA-S16-09; Design of Steel Structures, National Standard of Canada. Canadian Standard Association: Mississauga, ON, Canada, 2009.
17. Helwig, T.A.; Frank, K.H.; Yura, J.A. Lateral-torsional buckling of singly symmetric I-beams. *J. Struct. Eng.* **1997**, *123*, 1172–1179. [[CrossRef](#)]
18. Lamb, A.W.; Eamon, C.D. Load height and moment factors for doubly symmetric wide flange beams. *J. Struct. Eng.* **2015**, *141*, 04015069. [[CrossRef](#)]
19. Park, N.H.; Kang, Y.J.; Jo, Y.M.; Lim, N.H. Modification of C-equation in the SSRC Guide for buckling of monosymmetric I-beams under transverse loads. *Eng. Struct.* **2007**, *29*, 3293–3300. [[CrossRef](#)]
20. Bijak, R. The lateral buckling of simply supported unrestrained bisymmetric I-shape beams. *Arch. Civ. Eng.* **2015**, *61*, 127–140. [[CrossRef](#)]
21. Trahair, N.S.; Bradford, M.A.; Nethercot, D.A.; Gardner, L. *The Behaviour and Design of Steel Structures to EC3*, 5th ed.; Taylor & Francis: London, UK; New York, NY, USA, 2008.
22. Park, J.S.; Stallings, J.M. Lateral-torsional buckling of stepped beams with continuous bracing. *J. Bridge Eng.* **2005**, *10*, 87–95. [[CrossRef](#)]
23. Park, J.S. Lateral buckling formula of stepped beams with length-to-height ratio factor. *Struct. Eng. Mech.* **2004**, *18*, 745–757. [[CrossRef](#)]
24. Panedpojaman, P.; Sae-Long, W.; Chub-uppakarn, T. Cellular beam design for resistance to inelastic lateral–Torsional buckling. *Thin-Walled Struct* **2016**, *99*, 182–194. [[CrossRef](#)]
25. Ferreira, F.P.V.; Rossi, A.; Martins, C.H. Lateral-torsional buckling of cellular beams according to the possible updating of EC3. *J. Constr. Steel Res.* **2019**, *153*, 222–242. [[CrossRef](#)]
26. Sonck, D.; Belis, J. Lateral–torsional buckling resistance of cellular beams. *J. Constr. Steel Res.* **2015**, *105*, 119–128. [[CrossRef](#)]
27. Ferreira, F.P.V.; Tsavdaridis, K.D.; Martins, C.H.; De Nardin, S. Buckling and post-buckling analyses of composite cellular beams. *Compos. Struct.* **2021**, *262*, 113616. [[CrossRef](#)]
28. Khatri, A.P.; Katikala, S.R.; Kotapati, V.K. Effect of load height on elastic buckling behavior of I-shaped cellular beams. *Structures* **2021**, *33*, 1923–1935. [[CrossRef](#)]
29. Timoshenko, S.; Gere, J.M. *Theory of Elastic Stability*; McGraw-Hill International Book Company: New York, NY, USA, 1961.
30. Salvadori, M.G. Lateral buckling of I-beams. *Trans. Am. Soc. Civ. Eng.* **1955**, *120*, 1165–1177. [[CrossRef](#)]
31. ABAQUS/CAE, Version 6.20, Dassault Systèmes: Johnston, RI, USA, 2020.
32. Surla, A.S.; Kang, S.Y.; Park, J.S. Inelastic buckling assessment of monosymmetric I-beams having stepped and non-compact flange sections. *J. Constr. Steel Res.* **2015**, *114*, 325–337. [[CrossRef](#)]
33. Nguyen, X.T.; Park, J.S. Nonlinear buckling strength of steel H-beam under localized fire and pure bending. *KSCE J. Civ. Eng.* **2021**, *25*, 561–573. [[CrossRef](#)]
34. Nguyen, X.T.; Park, J.S. Design equations for buckling strength of steel I-beam under non-uniform heating condition. *Fire Saf. J.* **2022**, *127*, 103464. [[CrossRef](#)]
35. Gao, F.; Hu, B.; Zhu, H.P. Parametric equations to predict L_{JF} of completely overlapped tubular joints under lap brace axial loading. *J. Constr. Steel Res.* **2013**, *89*, 284–292. [[CrossRef](#)]
36. Gao, F.; Hu, B.; Zhu, H.P. Local joint flexibility of completely overlapped tubular joints under in-plane bending. *J. Constr. Steel Res.* **2014**, *99*, 1–9. [[CrossRef](#)]
37. Gao, F.; Hu, B. Local joint flexibility of completely overlapped tubular joints under out-of-plane bending. *J. Constr. Steel Res.* **2015**, *115*, 121–130. [[CrossRef](#)]
38. TCVN7571-16:2017; Hot-Rolled Steel Sections—Part 16: H Sections. Ministry of Science and Technology: Hanoi, Vietnam, 2017. (In Vietnamese)

Disclaimer/Publisher’s Note: The statements, opinions and data contained in all publications are solely those of the individual author(s) and contributor(s) and not of MDPI and/or the editor(s). MDPI and/or the editor(s) disclaim responsibility for any injury to people or property resulting from any ideas, methods, instructions or products referred to in the content.